

## Optical Variability of the Young Stellar Object GM Aurigae

Paige Romero  
University of New Mexico

### Abstract

A new wide-field imaging photometry technique was used to obtain high cadence, high precision, multicolor observations of a many stars field in the Taurus-Auriga molecular cloud. These observations were made with the goal of measuring the variability of stars suspected of planetary formation. We observed these objects at a higher cadence than previously accomplished. These observations reveal new, low-amplitude variability in the B bandpass with characteristic timescale of 30 minutes in the light curve of the well-studied T Tauri star GM Aur. We compare our observations of GM Aur with those previously obtained. We find long period variability on timescales of days to be consistent with previous observations. Our high cadence photometry reveals variability in the blue bandpass filter (B) that is not replicated in the V, R, or I filter bands. No previous observations report this kind of short timescale variability.

### Introduction

One of the major questions that modern astronomy seeks to resolve is that of origins - from the birth of the universe to the development of intelligence. A critical step in the solution is the frequency of formation of planets. The sheer number of extrasolar planets discovered and the frequency of pre-main sequence stars that show planetary formation indicate that planetary formation is a near universal phenomenon,(Haisch 2001). Despite its importance in the question of origins and its universal nature planetary formation is still not well understood.

It has been determined that nearly all stars ( $\geq 80\%$ ) form with a protoplanetary disk or circumstellar accretion disk, the consequence of conservation of angular momentum (Haisch 2001). It is within these disks that planets appear to form. Through direct imaging and indirect observations of extrasolar debris disks, disks similar to our Sun's asteroid belt and Kuiper belt, we are able to conclude that planetary formation is complete by  $\sim 12$  Myr after the stars form (Zuckerman and Song 2004). After 10-12 Myr regions of the protoplanetary disk where terrestrial and Jovian planets orbit are relatively devoid of warm dust (Strom et al. 1989). This indicates that the primary era of planetary formation has subsided. To study planetary formation it is necessary to make observations of stars that still retain their optically thick circumstellar disk. Stars that are observed to retain their protoplanetary disks are cataloged as either T-Tauri or Herbig Ae/Be stars. These stars are collectively considered Young Stellar Objects (YSOs).

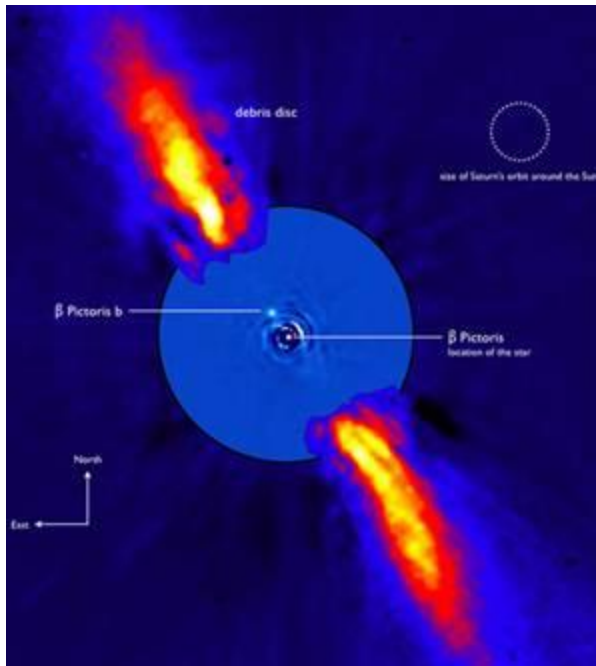


**Figure 1**

This ESO composite image of the southern hemisphere star  $\beta$  Pictoris shows the dusty debris disk at large distance from the star. The debris disk continues inward but is blocked at the boundary of the inner image of the composite. The inner (light blue background) image made at the VLT uses coronagraphic techniques to block the bright image of the star and simultaneously produce an image of the planet  $\beta$  Pictoris b. This system provides a conceptual model for recently formed protostars with debris disks in which planets might coalesce

(A.-M. Lagrange et al., European Southern Observatory/Science Photo Library)

Intensity and color variations in YSO light curves were expected and can be complicated. Some type of coalescence of material in the protoplanetary disk must occur during planetary formation. Thus, it is possible to measure disk density and compositional anisotropies to put constraints on planetary formation (Löhne, 2008). Evolution of the planet-forming debris disk of interacting gas, dust, and colliding planetesimal-like objects can include mechanisms such as physical and optical depth thickening as coalescence is initiated. Annuli of the disk in which planets form can be cleared both by accretion onto planetesimals (and ultimately onto the body of a planet) as well as by resonance effects. Modulation of the physical structure of the debris disk can create a variety of optical and infrared (OIR) intensity variations with a strong dependence upon the inclination of the disk to our line of sight. Density enhancements directly illuminated by starlight can modulate the total intensity by scattering. While transiting the star, density enhancements can appear in absorption and enhanced scattering. Absorption can create reddening (Grinin 1998). Transits of planets produce unique light curve signatures. As the protoplanetary nebula is condensing there is accretion of disk material. This creates emission in  $H\alpha$  (Muzerolle et al. 2000), in the IR spectral region (Beristain et al. 2001), in the UV (Herczeg et al. 2005), and in X-rays (H. M. Günther 2007). In short, debris disks surrounding YSOs are capable of modulating the OIR light curve of the star in complex ways. Comprehensive OIR observations of spectral line and continuum variability and descriptions of variability mechanisms can found in Sitko et al. (2008, 2011 and references therein).

There has been little done using high cadence optical photometry on this kind of star system. Using GM Aur as an example of how to study planetary formation in YSO's we demonstrate that our hypothesis that high cadence high-precision, multi-bandpass photometry is a required element for understanding planetary formation in YSOs, in general.

## Previous observations of GM Aur.

GM Aur is a known UX Ori variable, a subclass of YSO showing strong intensity and polarization variability. It was verified to have a circumstellar disk through submillimeter measurements done by Adams et al. in 1990 as part of a follow up to IRAS observations that had the sensitivity necessary to see blackbody emission from the debris disk. The geometry and density of the dust cloud has been estimated by Koerner et. al. (1992). Long period optical variation was measured by Bouvier et. al. in 1993. This revealed a rotational period of 12 days that was associated with spots on the surface. Stapelfeldt et al. released in HST WFPC2 IDT Hubble images that indicate a disk at a  $60^\circ$  inclination. There have been a number of models of the disk that appears present in GM Aur (Hueso 2002 and references therein). These models are currently not unique however, and require more observational constraints to better describe planetary formation. The Spitzer spectrograph verified another source of emission. GM Aur was observed to be accreting a small amount of material,  $\sim 0.02$  Lunar masses per year (Calvet, N., et al. 2005). This was previously suspected from the UV and X-ray observations. The Spitzer spectrograph also uncovered a gap in the disk that could very well be associated planetary formation.

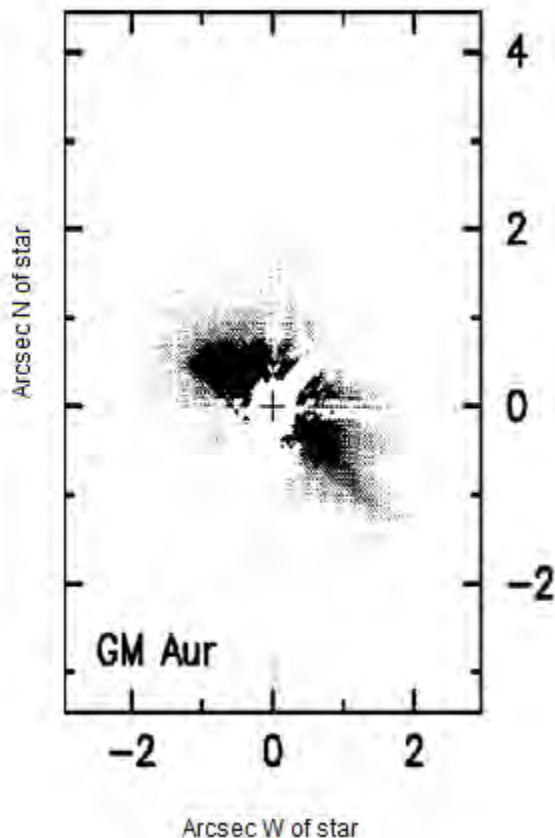


**Figure 2**

Hubble PC image of GM Aur taken in the R band. The point spread function of the star is removed in this image revealing a protoplanetary nebula around the star.

(Stapelfeldt 1997)

GM Aur is a well studied star. There is extensive evidence that it is a prime candidate for planetary formation. In spite of all the data gathered on it there are still few observational limits on the rate of planetary accretion in this system.

## Observations

Observations were originally taken with the goal of measuring the mass and distance to the parent star of a circumstellar density enhancement transiting the star. Our observations were made in a  $1^\circ \times 0.7^\circ$  field approximately centered on GM Aur in the Taurus-Auriga molecular cloud, a region containing many stars that have been observed to have a protoplanetary disk (Beckwith et al. 1990). One goal of this research is simultaneously to measure multiple YSOs using differential multicolor, high time resolution photometry measured relative to the same set of field (constant) comparison stars. With this technique we investigate YSOs as a class, yielding statistical information about the photometric signatures of different sub-types of YSOs and photometric differences among YSOs of the same sub-type. This is a new technique for the observation and statistical description of YSO variability.

To accomplish this set of observations we chose to use the 300mm f/5 Astromak astrograph which produces a  $3^\circ \times 3^\circ$  well-corrected field of view. This telescope, located at the UNM Campus Observatory (latitude  $35^\circ 5' 28''$ , longitude  $W106^\circ 37' 19''$ , altitude 1584m), used a Finger Lakes ML-6303E camera with a  $3072 \times 2048$  9 micron square pixel front-illuminated Kodak KAF 6303E CCD. This device has no anti-blooming, provides a linear full-well depth of nominally 100,000 electrons, a dark current of  $< 0.01$  electron/pixel/second at  $-35^\circ$  C, and a read noise of typically 10 electrons rms per read at a readout rate of 1 MHz.

The optical bandpass filters are a Bessell (1976, 1979) UBVRI set obtained from Omega Optics.

The optical field scale of the astrograph is 137.5 arcsec/mm. The nominal pixel scale is 1.24 arcsec, which reasonably samples the  $\sim 2 - 3$  arcsec FWHM seeing blurred PSFs provided by the Astromak astrograph. The active area of the CCD limits the observed field of view to  $1.05^\circ$  (RA)  $\times 0.70^\circ$  (DEC).

Previous observations of YSOs used telescope/camera configurations that typically provided a field of view of a few arcminutes, sufficient to measure a single YSO and several surrounding comparison stars. Our wide-field technique allows observation of multiple variable stars and many more (nominally constant brightness) comparison stars. This new observational technique allows simultaneous monitoring of multiple newly forming stars, most of which are luminosity variable, and an ensemble of reddened and unreddened comparison stars with which to robustly assess errors for differential photometry. The wide-field technique certainly provides observing efficiency and greater photometric precision, but perhaps more importantly it provides simultaneous monitoring of multiple types of YSOs to better assess physical sources of photometric variability amongst them.

In a star-forming region, many of the stars are YSOs of different subclasses, and many of those may be attempting to form planetary systems. Our field of view includes six known constant comparison stars which are used in the field as reference stars, and five suspected variables, four of which are of UX Ori-type variability. The UX Ori class of variable stars exhibits large photometric and polarimetric variations that are thought to be due to variable extinction by

circumstellar dust (Grinin 1994). Three of the stars in the field are known T-Tauri stars (Beckwith et al. 1990). The field, derived from an image made in the V filter on 2012 5 January is shown in Figure 3. Note that research reported here concentrates on the UX Ori-type YSO variable GM Aur labeled “1” in this image. Note, too, that future research will be devoted to the discovery of additional variable stars in this field, and confirmation of the constancy of the currently designated comparison stars and definition of other comparisons for comprehensive differential photometry of this entire field.

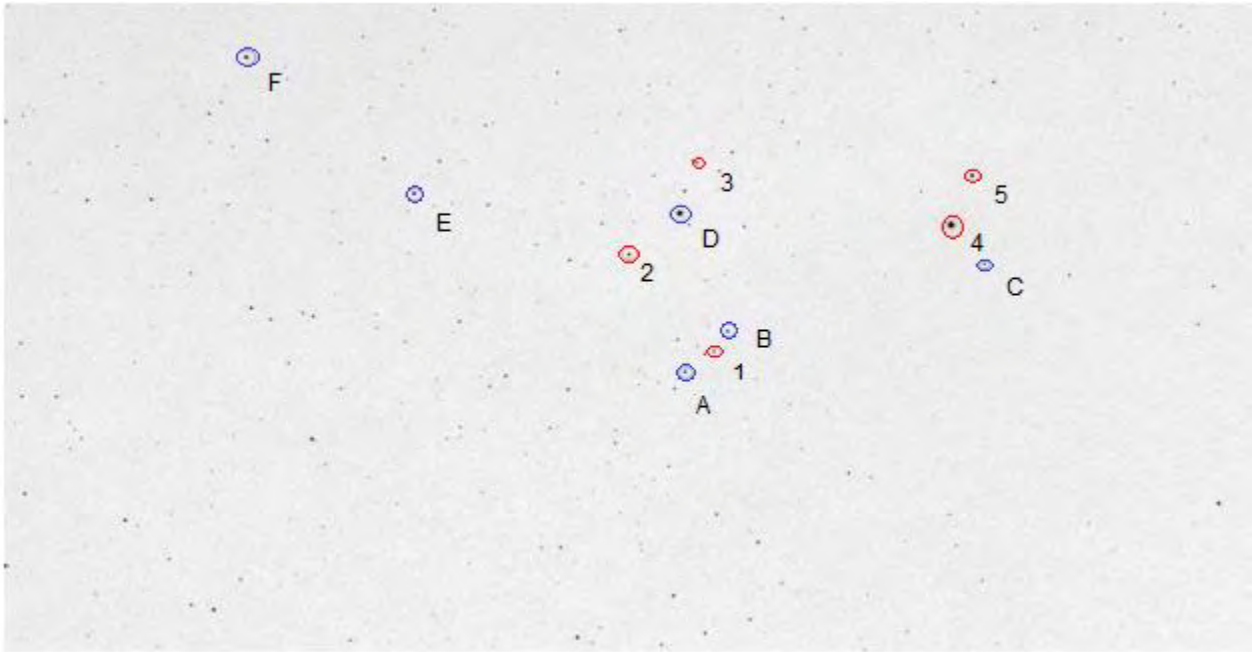


**Figure 3.** A typical image of the field of view for which data were obtained. Blue circles/letters indicate a star that was used as a reference. Red circles/numbers indicate a known variable.

Variables

Name	V Magnitude	Variable type	Spectral type	Notes
1. GM Aur	12.1	T Tauri	K5V	Primary target
2. V* 396 Aur	11.24	UX ori, T Tauri	K0V	
3. V* 397 Aur	11.46	UX ori, T Tauri	K5	
4. AB Aur	7.06	UX Ori	A0V	Planet detected
5. SU Aur	(B) 10.22	UX Ori	G2III	

Reference stars

A. HD 282626	11.7		F5	
B. HD 282625	10.9		G0	
C. JH 429	(B)11.8		~	
D. HD 31305	7.60		A0	
E. HD 282636	(B)9.4		F8	
F. HD 282635	9.75		B8	

High cadence time domain imaging photometry using BVRI filters was accomplished on the field. Individual measurement sequences (BVRI) were taken at near-constant intervals of

about six minutes, and spanned an interval of about three months. A total of 11 nights of data was taken of this field. This represents the highest cadence photometry done on these objects.

## Data Analysis

The data analysis procedure included removal of the instrumental signature by application of flat field, dark and bias CCD frames.

### a) Instrumental signature removal and throughput correction

Raw data were bias subtracted, flat field corrected, and overscan corrected using MATLAB routines written by Dr. Peter Zimmer. The data were not corrected for dark current because the dark current is sufficiently low that correcting for it would have introduced more error than neglecting it.

### b) Astrometric Solutions

Individual data frames require registration to ensure light curves and colors refer to the same stars. The registration is supplied by accomplishing an astrometric translation/rotation solution for each frame relative to an astrometric catalog. Astrometric solutions were applied to each image using the program “The SkyX.” This software program used a map of the sky and fit a central field position and orientation based on the pixel scale. The output generated was entered into the FITS header of each image.

### c) Photometry

Aperture photometry was done using Source Extractor (SExtractor) (Bertin and Arnouts 1996). The algorithm fit an inner annulus around each star and found a sum of incident counts from each star. This was corrected for background counts by subtracting a background value found from integrating an outer ring around the annulus surrounding each star. The radius of the photometric inner circle, the guard annulus and the background evaluation annulus was determined empirically. Each star had an instrumental flux, error, and position associated with it. The position was calculated from the header information that was supplied by The SkyX.

### d) Propagation of Errors

All error in all filters was derived from shot noise and read noise using algorithms supplied by SExtractor. The propagation of error from taking the ratio to reference stars was calculated through the relation

$$\frac{\sigma_f^2}{f^2} = \frac{\sigma_A^2}{A^2} + \frac{\sigma_B^2}{B^2}$$

where

$$f = \frac{A}{B}$$

A is the flux of star of interest and B is the flux of the reference star. Each  $\sigma^2$  is the variance of each term respectively. Measurement errors were calculated for every star measurement.

#### e) Light Curves

Light curves were then generated by using MATLAB to rearrange the SExtractor output to have each star in each exposure associated with the correct star from the previous exposure. This method of list sorting was based on finding the minimum distance of each star to a mean position defined by all earlier exposures. To correct for atmospheric effects the method of differential photometry was employed. The instrumental flux of each star was divided by that of the nearest reference star.

#### f) Reference Stars

Each reference star was identified by sky position taken from the AAVSO catalog of reference stars. Using the method of differential photometry amongst all reference stars allowed verification that each star was sufficiently constant (rms variations less than 0.1%).

### **Detection and Discovery of Variability**

#### a) Long Term Variability

We have verified that there is long term variability within GM Aur. This variability is consistent with the previously measured long-term periodicity of this star.

When long term variability in the V filter was compared to the previously measured rotational period of 12 days (Bouvier 1993) we found our data were consistent with these results.

It is clear that there are other enhancements and dips in the lightcurve that cannot be modeled with a simple single sinusoid. These are the kinds of unresolved features that lead to errors when doing low cadence photometry. The bump on 6 January is an example of this. This enhancement in the V exists in all other filters. The color variation over this night is negligible. With future, more closely spaced and more complete data we plan to accomplish a complete Fourier analysis of the variability of this and other YSOs in this field.

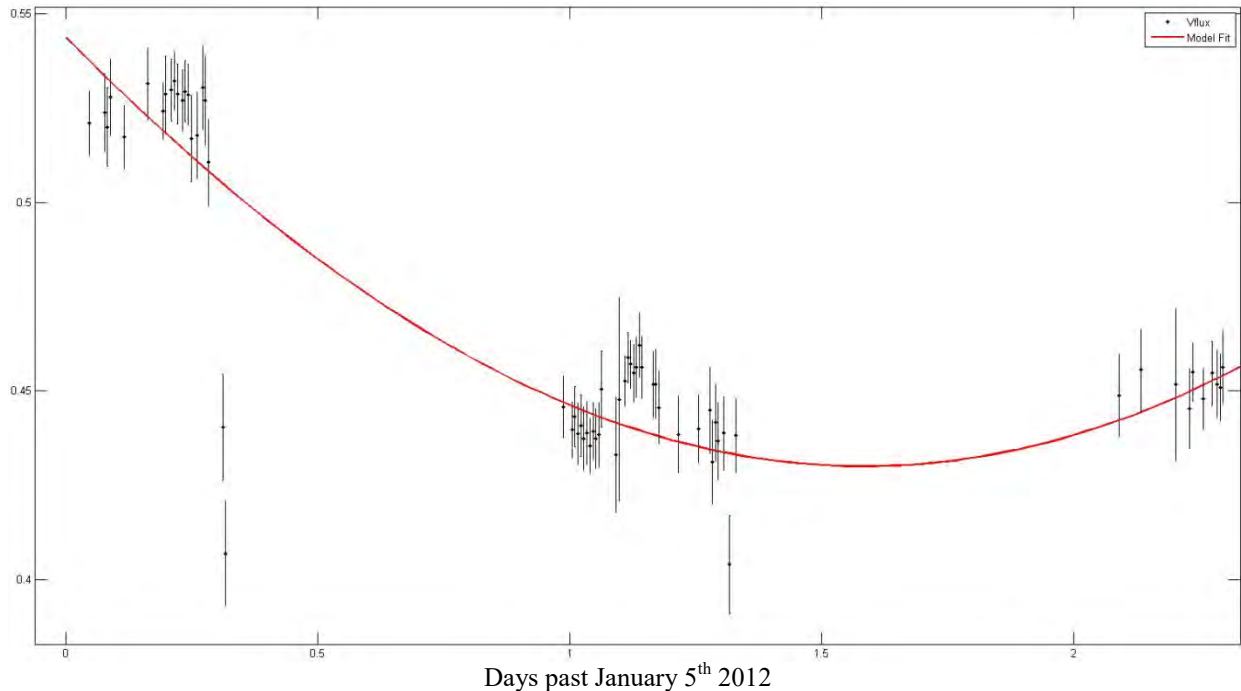


**Figure 4** Three nights of observation of GM Aur in the V filter compared to the best fit for a single sinusoid with a period of 12 days. This period is consistent with previous observation of GM Aur that attribute this variation to a rotational period. Note that variability within each night is also apparent.

#### b) Discovery of Short Term Variability in GM Aur

The instrumental B-V measured for GM Aur measured on nearly all the nights was between 0.6 and 0.8 (instrumental colors). On 25 January 2012 the instrumental B-V decreased (became redder) in two distinct minima of about 0.4 magnitude in depth. This is attributed to observing two distinct dips in the B magnitude of GM Aur.

The following color and intensity light curves demonstrate the effect. Color in instrumental (B-V) magnitudes is plotted vertically vs. time on the night of 25 January 2012.

The comparison of color of GM Aur variations is shown for three different comparison stars in order to demonstrate that the color variation appears to exist only in the blue (B filter). The use of nearby reference stars (see Figure 3) precludes atmospheric effects as the cause of B variability, and the appearance of this curve relative to a multiplicity of comparison stars shows that this variation is due to activity within GM Aur itself, and not one of the comparison stars.

We are able to conclude that this is a decrease of intensity in the B filter, rather than an enhancement, by examining the B magnitude of GM Aur on the previous nights. When we do this we see that the B is similar to the peak of the B from 25 January. It is important to determine the nature of the variability to allow for the appropriate interpretation of the physical mechanism of variability. T Tauri stars are known to exhibit enhancements in the blue due to variable



accretion of material on the surface of the star. We conclude that this is a dip in the blue and in only the blue.

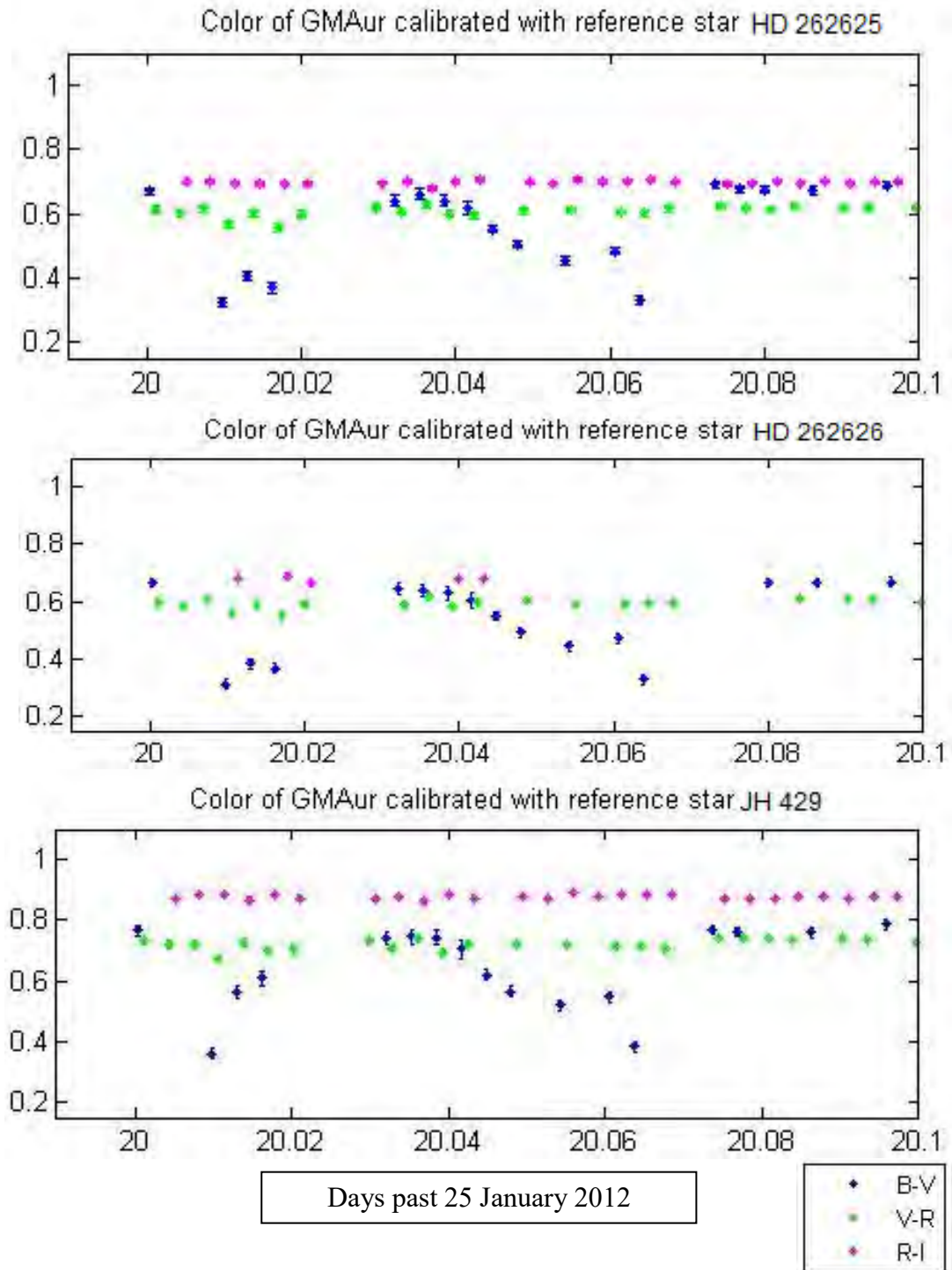


**Figure 5** Instrumental color of GM Aur with intensities corrected using three different reference stars. Note: certain points are missing from the curves due to aggressive exclusion of variations in the astrometric solutions for each exposure.

It is clear that this dip is indeed a real effect and is attributable to activity within GM Aur. We have shown that the same effect is seen when calibrating GM Aur to three different reference stars, two of which are in close proximity to GM Aur. This allows us to rule out the potential of atmospheric fluctuations or variability in a comparison star as causing the dip. If atmospheric fluctuations were to occur they would not affect the entire wide field of view and they would have affected all colors. Stars with a close angular proximity would be obscured by approximately the same amount of atmospheric extinction, which is not observed. If there were variability in the reference stars then it would be seen in only one of the reference stars. We conclude that the observed variation in the B bandpass of the GM Aur light curve is real, that it represents diminution of B light, and that whatever the cause of the diminution is not a broadband effect because the modulation is not seen within the error bars of the lights curves in other bandpasses.

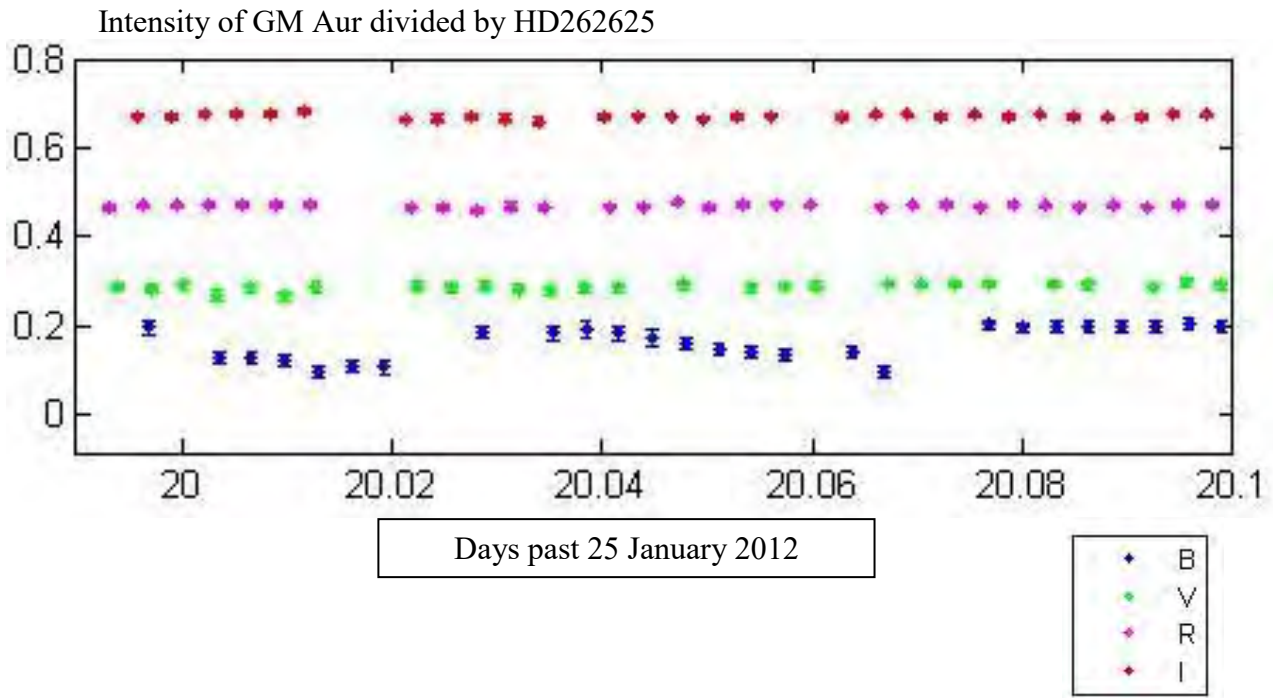


**Figure 6** The relative flux of GM Aur corrected with the nearest reference star. The change in color can be attributed to the dip in the blue alone. The depth of each dip appears to be  $\sim 30\%$ . There seems to be no detectable dip in any of the other filters.

We do not see any significant dip in either of the other filters. Variable Rayleigh scattering in the clumpy gas component of the disk of GM Aur has been suggested as a source of strong blue variability, in general. We find that this change cannot be explained by the  $\lambda^{-4}$  dependence of the dominating term in scattering cross section in Rayleigh scattering.

## A Simple Scattering Model

Other color dependent variability that has been observed in Ux Ori spectral type stars has been attributable to Rayleigh scattering. We find that this is not the case for the dip in the B filter that we observe for GM Aur. Other studies have found fluctuations in the V band associated with the deep dip in the blue. We do not observe any dip in the V filter.

We do a test to verify that the strong wavelength dependence does not just push the variability below the error bars in the other filters.

We employ a simplified model of Rayleigh scattering:

$$\frac{I}{I_0} = e^{-n\sigma_\lambda s}$$

This equation predicts the ratio of light transmitted through an obscuring density enhancement (forward scattering) to the amount of light incident on the matter, where  $n$  is the column density of particles,  $\sigma_\lambda$  is the scattering cross section, which is a function of wavelength, and  $s$  is the thickness of the material.

The fractional depth of the dip is

$$f(\lambda) = \frac{I_0 - I}{I_0}$$

or

$$f(\lambda) = 1 - e^{-n\sigma_\lambda s}$$

Because the process in question is Rayleigh scattering for a column of gas, we expect

$$\sigma_\lambda \propto \lambda^{-4}$$

where  $\sigma$  is a constant related to the scattering cross section and that depends on the composition of the gas cloud from which the starlight is scattering.

So

$$f(\lambda) = 1 - e^{-n\sigma s \lambda^{-4}}$$

where  $n\sigma s$  is a constant that we fit to best describe the dip in the light curve.

Fitting for the amount of change in the wavelength associated with the maximum filter throughput for each filter we get an estimate of  $n\sigma s$ . This in turn gives us what we should expect as a change in the other bandpasses if the source of the obscuration was just Rayleigh scattering.

If we choose  $n\sigma \sim 12.2E9$ :

**Table 2** Fractional change through each filter that best explains the dip in the B band and no noticeable dip in any other filter bandpass.

Filter	B	V	R	I
Fractional change	0.300	0.134	0.096	0.0308

The predicted fractional change through V, R, and I are much higher than their respective error bars, so were there variability corresponding to that we observe in B, we should detect it.

Because we do not detect variability corresponding to that observed in B in any other bandpasses, we have shown that this variation cannot be attributed to Rayleigh scattering alone. This dip is unlike any that has been discussed in any other study done on this kind of star. High cadence high precision photometry has led to a discovery in the B color variability of GM Aur.

It would have been very useful to have taken exposures in the U filter. This would have led us to make conclusions on the nature of this variation as spectral line variability or strongly wavelength dependent continuum variability.

It is possible that this dip may be related to a monochromatic mechanism, e.g. line emission in the B bandpass, associated with disk accretion. Alternatively, this could be caused by a broadband mechanism extending blueward that might have been observed had we utilized the U bandpass of the Bessell filter set. We anticipate using the U bandpass on future observations, though the throughput of this filter is poor leading to long integration times. It is still unclear what mechanism that can cause variation in the blue visible range alone, though this intriguing result might help refine the complicated disk models currently used to describe planetary formation in YSO systems.

## Conclusions

For GM Aur we have confirmed night-to-night variability with a period of  $\sim 12$  days that is consistent with previous observations. We have discovered that there is intra-night variability that exists only in the B filter band. It is unclear whether this is due to continuum variability of spectral line variability. We have demonstrated that it is necessary to make high cadence high precision photometric observations in order to achieve a strong understanding of planetary formation. Wide field imaging photometry of star forming regions for which many, relatively bright variable YSOs of various sub-classes can be simultaneously observed provides a useful technique for future observing programs.

## References

- Appenzeller, I.; Mundt, R., 1989 A&ARv...**1**..291A.  
Beckwith, Steven V. W. et al. 1990AJ....**99**..924B.  
Beristain, G., Edwards, S., & Kwan, J. 2001, ApJ, **551**, 1037.  
Bessell, M. S. 1976 PASP **88**, 557  
Bessell, M. S. 1979, PASP **91**, 589.  
Bertin, E. and Arnouts, S. 1996, A&A Supplement **317**, 393.  
Bouvier, J.; Cabrit, S.; Fernandez, M.; Martin, E. L.; Matthews, J. M. 1993A&A...**272**..176B.  
Bouvier, J.; Covino, E.; Kovo, O.; Martin, E. L.; Matthews, J. M.; Terranegra, L.; Beck, S. C.,  
1995A&A...**299**...89B.  
Calvet, N., et al. 2005, ApJ, **630**, L185.  
Chiang, E. I.; Goldreich, P., 1997ApJ...**490**..368C.  
Covey, K et. al. 2010, arXiv:1012.3732v1.  
Dalgarno, A. & Williams, D. A., 1962ApJ...**136**..690D.  
Donati, J.-F., et. al. 2007MNRAS.**380**.1297D.  
Dutrey, S. Guilloteau, L. Prato, M. Simon, G. Duvert, K. Schuster, and F. M'énard, 1998,  
Astron. Astrophys. **338**, L63–L66 (1998)  
Espaillat, C. et al, 2010ApJ,**717**,441E.  
Gomez, M. et al, 1992AJ....**104**..762G.  
Grinin, V. P., 1994A&A...**292**..165G.  
Grinin, V. P.; Rostopchina, A. N.; Shakhovskoi, D. N., 1998AstL...**24**..802G.  
H. M. Günther, J. H. M. M. Schmitt, J. Robrade, and C. Liefke, 2007A&A...**466**.1111G  
Haisch, Karl E., Jr., 2001 ApJ...**553L**.153H.  
W. Herbst, 1999 AJ, **118**,1043.  
Herczeg, Gregory J. et al., 2005 AJ....**129**.2777H.  
Hueso, R.; Guillot, T 2005 A&A...**442**..703H.  
Hueso, R. N et. al., 2002 DPS....**34**.2801H.  
Hughes, A. et al. 2009 ApJ, **698**, 131H.  
Joy, Alfred H. 1945 ApJ...**102**..168J.  
Koerner et. al, 1992 AAS...**181**.5807K.  
Leisenring, Jarron; Bary, J.; Skrutskie, M., 2007 AAS, **211**.6212L.  
Löhne, Torsten; 2008 ApJ...**673**.1123L.  
Motohide, T., et. al, 1999ApJ...525..832T  
Muzerolle, J., Calvet, N., Briceño, C., Hartmann, L., & Hillenbrand, L. 2000,  
ApJ, **535**, L47.  
Percy, John R.; Grynko, Sergiy; Seneviratne, Rajiv; Herbst, William, 2010 PASP..**122**..753P.  
Stapelfeldt, K., WFPC2 Science Team 1997 svlt.work..395S.  
Strom, K.M., et al. 1989, AJ, **97**, 1451.  
Wyatt, Mark C. 2008ARA&A..**46**..339W.  
Zuckerman, B. Song, I. 2004, ARA&A, **42**, 685.